Design and Investigation of Fuzzy-PI and RST Controllers for a High Performance Matrix Converter Using Venturini Modulation Strategy Under Distorted Grid Voltage

B. Hamane[1, 3], M. L. Doumbia[1], H. Chaoui[2], A. Chériti[1], M. Bouhamida[3], and M. Benghanem[3]
[1]Dept. of Electrical and Computer Engineering, Université du Québec à Trois-Rivières, QC, Canada
bekhada.hamane@uqtr.ca; mamadou.doumbia@uqtr.ca; ahmed.cheriti@uqtr.ca
[2]Center for Energy Systems Research, Department of ECE, Tennessee Technological University, Cookeville, TN, USA
hchaoui@tntech.edu
[3]Dept. of Electrical Engineering, University Mohamed Boudiaf, Oran, Algeria
m_bouhamida@yahoo.com; mbenghanem69@yahoo.fr

Abstract— **The purpose of this paper is to design and control the load's current of a Matrix Converter (MC) using both Fuzzy-PI and RST controllers in terms of tracking the reference and robustness. RST controllers present a time delay on the system's transient response. This technique is known to offer lower performance when it is used in complex and nonlinear systems. On the other hand, fuzzy-PI control offers better performance, even in case of highly nonlinear systems. In this paper, a Fuzzy-PI control strategy is proposed as an output current controller to improve the performance of the MC powered by unbalanced and distorted grid voltages. The overall operating principle, Venturini modulation strategy of MC, Fuzzy-PI control and characteristics of RST control are presented. Our investigation shows that the Fuzzy-PI can give better performance to overcome the limitation of RST control in nonlinear systems. To show the effectiveness of the control methods, the performance of the system is analyzed and compared in various operating conditions.**

Keywords- Matrix Converter; Distorted Grid; Venturini Modulation Strategy; Fuzzy-PI Control; RST Control

I. INTRODUCTION

Recent advances in power electronics have enabled the emergence of Matrix Converter (MC) for direct AC/AC conversion [1]. Interest in this converter topology was rather academic with efforts provided in many research laboratories [1]. The basic diagram of a MC is represented in Fig. 1. It uses bidirectional current and voltage power switches that connect converter input and output phases [2], which are used to directly connect the power supply to the load without using any DC-link or large energy storage elements [2, 3]. The clipping circuit is used to protect the converter against surges which could come from a sudden disconnection of the load [1]. MC was introduced firstly in 1976. To prevent the spread of current harmonics caused by the MC to the supply network, an input LC filter is used. It provides a very low impedance path and absorbs current harmonics [1, 2]. Venturini and Alesina proposed in 1980 a generalized high-frequency switching strategy [3]. The objective of this control strategy is to achieve an ideal electronic transformer capable of varying the voltage, current, frequency and power factor [4]. Another method, known as the direct transfer function approach, proposes the multiplication of the input voltages vectors by the modulation matrix M to obtain a vector of output voltages which correspond to a point of synthesis [4]. However, the simultaneous commutation of controlled bidirectional switches used in MC is very difficult to achieve without generating overcurrent or overvoltage spikes which can destroy the power semiconductors [3]. Also, the load side of the MC is directly affected by the distorted and/or unbalanced input voltages due to the lack of DC intermediate circuit in the MC. The performance of the MC deteriorates, when it is exposed to the harmonic and non-sinusoidal currents and some papers have been presented mitigation methods [3, 5]. Conventional PI controller works well only if the mathematical model of the system could be computed. However, it is difficult to implement the conventional PI controller for variable as well as complex systems [5]. So, Fuzzy Logic Controller (FLC) which does not require any precise mathematical model and gives good response for complex applications can be applied. The Fuzzy-PI based controller is capable to embed the qualitative knowledge and experience of an operator or field engineer about the process [7]. In this paper, RST Controller is investigated. This regulator, whose synthesis is purely algebraic, is a sophisticated algorithm based on the pole placement method which exploits many numerical resources [7, 16]. This work presents theoretical analysis, modeling, and an in-depth comparison of both the Fuzzy-PI and RST Controllers for MC. Results show the superiority of the Fuzzy-PI strategy with faster dynamic response and better robustness.

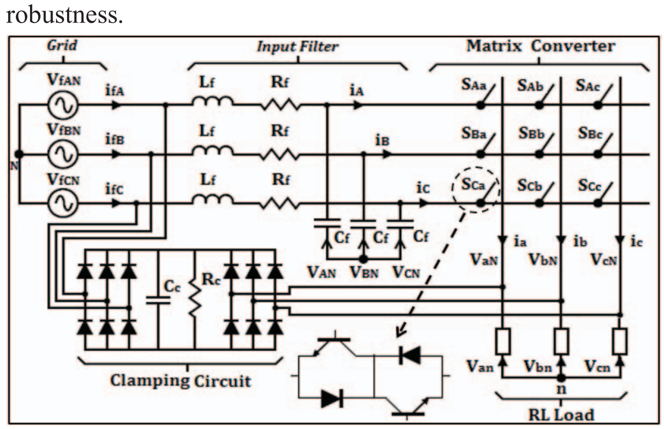

Figure 1. Basic circuit of a Matrix Converter

II. MATHEMATICAL MODEL OF MATRIX CONVERTER

This part consists of a brief description and modeling of each element of the matrix converter. We start with modeling the MC and the input filter. Ideal bidirectional switches are represented by S_{ij}, where $i = \{A,\ B, C\}$ and $j = \{a,\ b, c\}$ represent respectively the index of input and output voltage [1, 9]:

$$S_{ij} = \begin{cases} 1 & \text{If the switch } S_{ij} \text{ is closed} \\ 0 & \text{If the switch } S_{ij} \text{ is opened} \end{cases} \quad (1)$$

$$S_{Aj} + S_{Bj} + S_{Cj} = 1 \quad (2)$$

With these restrictions, a 3×3 matrix converter has 27 possible switching states [1]. Let m_{ij} be the duty cycle of switch S_{ij}, defined as [1]:

$$m_{ij}(t) = \frac{t_{ij}}{T_{seq}} \quad (3)$$

Where: $0 < m_{ij} < 1$, $T_{seq} = \frac{1}{f_s}$

The transfer matrix of the converter is defined by [1, 3]

$$M = \begin{bmatrix} m_{Aa} & m_{Ba} & m_{Ca} \\ m_{Ab} & m_{Bb} & m_{Cb} \\ m_{Ac} & m_{Bc} & m_{Cc} \end{bmatrix} \quad (4)$$

A. Modeling of the Matrix Converter

The input voltage and current of the matrix converter are given by [1, 10]:

$$V_i = V_{im} \begin{bmatrix} \cos(\omega_i t) \\ \cos\left(\omega_i t + \frac{2\pi}{3}\right) \\ \cos\left(\omega_i t + \frac{4\pi}{3}\right) \end{bmatrix} \quad (5)$$

$$I_i = I_{im} \begin{bmatrix} \cos(\omega_i t + \varphi_i) \\ \cos\left(\omega_i t + \varphi_i + \frac{2\pi}{3}\right) \\ \cos\left(\omega_i t + \varphi_i + \frac{4\pi}{3}\right) \end{bmatrix} \quad (6)$$

The matrix converter will be designed and controlled to provide desired output voltage and output current [1, 10]:

$$V_o = V_{om} \begin{bmatrix} \cos(\omega_o t) \\ \cos\left(\omega_o t + \frac{2\pi}{3}\right) \\ \cos\left(\omega_o t + \frac{4\pi}{3}\right) \end{bmatrix} \quad (7)$$

$$I_o = I_{om} \begin{bmatrix} \cos(\omega_o t + \varphi_o) \\ \cos\left(\omega_o t + \varphi_o + \frac{2\pi}{3}\right) \\ \cos\left(\omega_o t + \varphi_o + \frac{4\pi}{3}\right) \end{bmatrix} \quad (8)$$

The neutral to phase output voltages V_{aN}, V_{bN} and V_{cN} are given by [1, 3, 9]:

$$\begin{bmatrix} V_{aN} \\ V_{bN} \\ V_{cN} \end{bmatrix} = \begin{bmatrix} m_{Aa} & m_{Ba} & m_{Ca} \\ m_{Ab} & m_{Bb} & m_{Cb} \\ m_{Ac} & m_{Bc} & m_{Cc} \end{bmatrix} \begin{bmatrix} V_{AN} \\ V_{BN} \\ V_{CN} \end{bmatrix} \quad (9)$$

The input current I_A, I_B and I_C are [3, 9]:

$$\begin{bmatrix} I_A \\ I_B \\ I_C \end{bmatrix} = \begin{bmatrix} m_{Aa} & m_{Ab} & m_{Ac} \\ m_{Ba} & m_{Bb} & m_{Bc} \\ m_{Ca} & m_{Cb} & m_{Cc} \end{bmatrix} \begin{bmatrix} I_a \\ I_b \\ I_c \end{bmatrix} \quad (10)$$

ω_i, V_{im} are respectively the input voltage frequency and amplitude.

I_{im}, φ_i are respectively the input current amplitude and input phase.

ω_o, V_{om}, f_s are respectively the output voltage frequency, amplitude and the switching frequency.

Assuming the relationship between the output and the input signal of the matrix converter [1, 11]:

$$q = \sqrt{\frac{V_o^2}{V_i^2}} = \sqrt{\frac{I_i^2}{I_o^2}} \qquad \text{with: } 0 < q \leq 0.866 \quad (11)$$

B. Modeling of the Input Filter

The LC input filter is a series resonant circuit tuned to the frequency of harmonics and connected in shunt. It provides a very low impedance path and absorbs harmonic currents [1, 3]. At the fundamental frequency, the filter acts as a reactive power compensator [1, 3]. The LC input filter may be modeled with the equivalent circuit. From the Kirchhoff's laws, node equations and Laplace transformation, the equivalent circuit [1, 11] can be represented as shown in Figure 2.

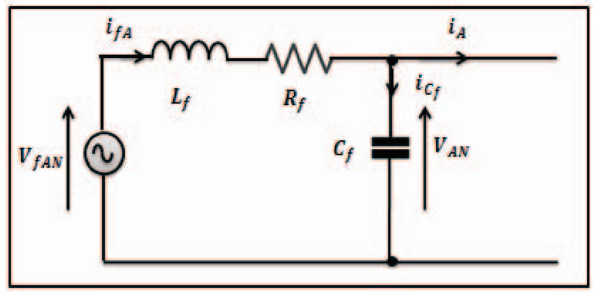

Figure 2. Input filter scheme

The filter output voltage and input current are obtained as equations 12 and 13 [1, 12].

$$V_{AN}(p) = \frac{1}{L_f C_f p^2 + R_f C_f p + 1} V_{fAN} - \frac{L_f p + R_f}{L_f C_f p^2 + R_f C_f p + 1} I_A \quad (12)$$

$$I_{fA}(p) = \frac{1}{L_f C_f p^2 + R_f C_f p + 1} I_A + \frac{C_f p}{L_f C_f p^2 + R_f C_f p + 1} V_{fAN} \quad (13)$$

III. CONTROL STRATEGY OF MATRIX CONVERTER

This strategy can produce the sinusoidal input current with unity power factor independently of load [4, 9]. The principle is to synthesize the desired three phase output voltage from the input voltage during each defined switching period.

The initial equations of Venturini method are obtained as the product the ratio q, the voltage amplitude, third harmonic frequency of the input and output voltage as indicated in references [3, 8]:

$$V_o(t) = qV_{im} \begin{bmatrix} \cos(\omega_o t) - \frac{1}{6}\cos(3\omega_o t) + \frac{1}{2\sqrt{3}}\cos(3\omega_i t) \\ \cos\left(\omega_o t + \frac{2\pi}{3}\right) - \frac{1}{6}\cos(3\omega_o t) + \frac{1}{2\sqrt{3}}\cos(3\omega_i t) \\ \cos\left(\omega_o t + \frac{4\pi}{3}\right) - \frac{1}{6}\cos(3\omega_o t) + \frac{1}{2\sqrt{3}}\cos(3\omega_i t) \end{bmatrix} \quad (14)$$

According to the optimal amplitude in expression of Venturini, the modulation function is [1, 8, 11]:

$$m_{ij} = \frac{1}{3}\left[1 + \frac{2V_i V_j}{V_{im}^2}\right] \quad (15)$$

Therefore, only six duty cycles are sufficient to calculate the gate signals of the power switches [10].

$$\left.\begin{matrix} X = t_{Aj} \\ Y = t_{Aj} + t_{Bj} \end{matrix}\right\} ==> \begin{cases} S_{Aj} = (X) \\ S_{Bj} = (\overline{X}) \text{ and } (Y) \\ S_{Cj} = (\overline{X}) \text{ and } (\overline{Y}) \end{cases} \tag{16}$$

The carrier signal is expressed by [10]:

$$U_p = \frac{1}{T_{seq}} t \qquad \text{with: } 0 \le t \le T_{seq} \tag{17}$$

IV. CONTROLLER DESIGN

This section deals with the design and synthesis of the Fuzzy-PI and RST controllers. Both controllers are designed to achieve current reference tracking with varying current reference signals. This has also to be achieved under balanced, unbalanced and distorted grid voltage conditions.

A. Fuzzy-PI Controller design

According to the operational features of matrix converter and control requirements, a Fuzzy-PI Control strategy was developed.

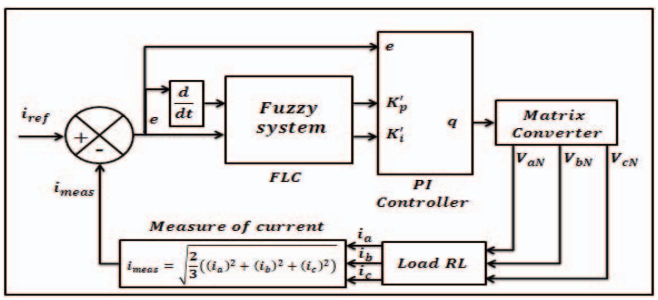

Figure 3. Control CM using Fuzzy-PI

The system's structure is shown in Figure 3. A Proportional Integral (PI) controller is used with fuzzy supervisory control system. Using the error signal and its derivative, the fuzzy system adjusts continuously the parameters of the PI controller to fit all operating conditions [17]. The diagram suggested by Mamdani [18] is used to develop the controller.

The input signals of fuzzy controller are the error (e) and its derivative (de/dt), and the output signals are the normalized value of the K'_p and the normalized value of the K'_i. The input signals have 7 membership functions, while the proportional gain K'_p has 2 and the integral gain K'_p has 3. The 7 membership functions of the inputs are designed as shown in Figure 4 (a), (b). The membership functions for the K'_p and the K'_i are designed as shown in Figure 4 (c), (d).

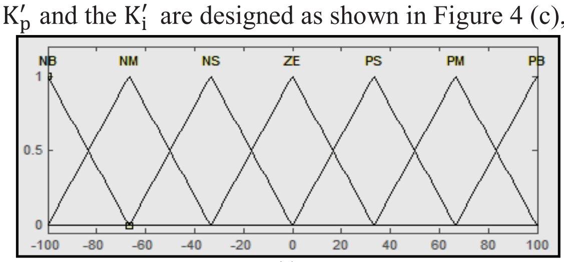

(a)

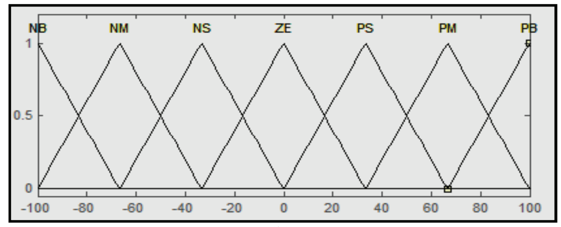

(b)

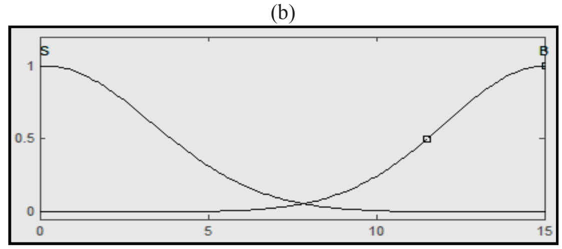

(c)

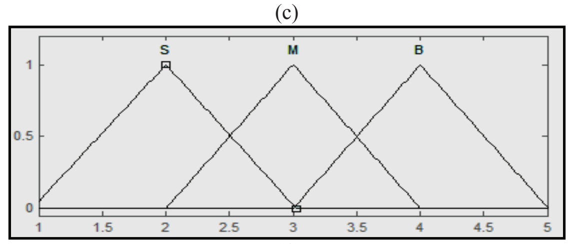

(d)

Figure 4. The membership functions of FLC

Big : B; Medium : M; Small : S; Negative Big : NB; Negative Medium : NM ; Negative Small : NS; Zero : ZE; Positive Small : PS; Positive Medium : PM; Positive Big : PB.

The center of gravity method [18] is used to defuzzify the output variable of the system:

$$u = \frac{\sum_{i=1}^{m} \mu(x_i).x_i}{\sum_{i=1}^{m} \mu(x_i)} \tag{18}$$

The other cases can be tuned by the same way. The rules tables of K'_p and K'_i are shown respectively in Table I and II.

TABLE I. FUZZY RULES FOR CONTROLLER COEFFICIENT K'_p

U		e						
		NB	NM	NS	ZE	PS	PM	PB
de	NB	B	S	S	S	S	S	B
	NM	B	B	S	S	S	B	B
	NS	B	B	B	S	B	B	B
	ZE	B	B	B	B	B	B	B
	PS	B	B	B	S	B	B	B
	PM	B	B	S	S	S	B	B
	PB	B	S	S	S	S	S	B

TABLE II. FUZZY RULES FOR CONTROLLER COEFFICIENT K'_i

U		e						
		NB	NM	NS	ZE	PS	PM	PB
de	NB	S	M	B	B	B	M	S
	NM	S	M	M	B	M	M	S
	NS	S	S	M	M	M	S	S
	ZE	S	S	S	M	S	S	S
	PS	S	S	M	M	M	S	S
	PM	S	M	M	B	M	M	S
	PB	S	M	B	B	B	M	S

The PI controller parameters are normalized in the interval $K_p \in [0, 15]$; $K_i \in [1, 5]$. Once the values K'_p and K'_i are obtained, the new parameters of the PI controller are calculated by the equation [17, 18]:

$$\begin{cases} K'_p = (K_p - K_{pmin})/(K_{pmax} - K_{pmin}) \\ K'_i = (K_i - K_{imin})/(K_{imax} - K_{imin}) \end{cases} \quad (19)$$

The reference current is calculated as shown in Fig. 5 [10].

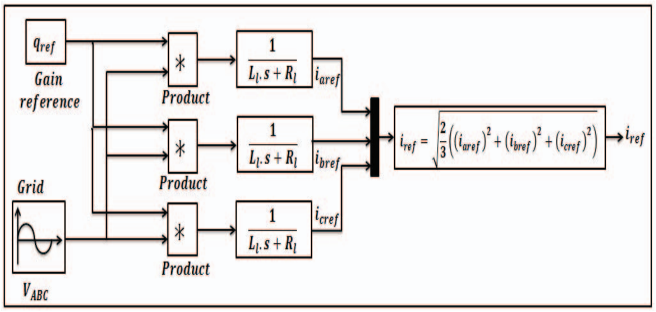

Figure 5. Load reference current

The measured load's and reference currents are given respectively by the equation (20) [10, 15]:

$$\begin{cases} i_{meas} = \sqrt{\frac{2}{3}((i_a)^2 + (i_b)^2 + (i_c)^2)} \\ i_{ref} = \sqrt{\frac{2}{3}((i_{aref})^2 + (i_{bref})^2 + (i_{cref})^2)} \end{cases} \quad (20)$$

B. *RST Controller design*

The goal of this section is to determinate the RST controller's current. This type of controller is a structure with two freedom degrees and compared to a one degree of freedom structure, it has the main advantage that it allows the designer to specify performances independently with reference trajectory tracking (reference variation) and with regulation [7, 8]. The closed-loop system of the RST controller for MC is given by the following block diagram (Fig. 6).

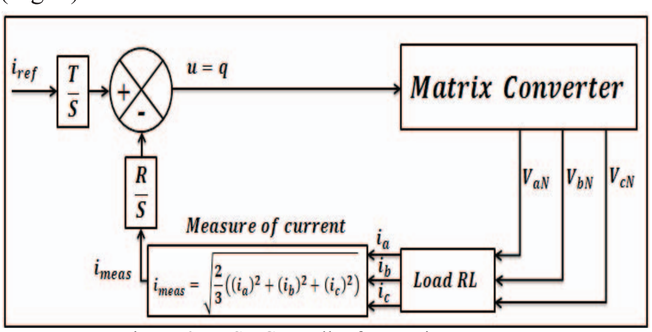

Figure 6. RST Controller for matrix converter

It is based on the pole placement theory [16], which consists in specifying an arbitrary stability polynomial D(p) and calculate S(p) and R(p) according to the Bezout equation [7, 8]:

$$D = AS + BR \quad (21)$$

With:

$$\deg(D) = \deg(A) + \deg(S) \quad (22)$$

The transfer function of the system is:

$$T(p) = \frac{B}{A} = \frac{1}{R_l + L_l p} \quad (23)$$

For our model, we obtain [8]:

$$\begin{cases} A = a_1 p + a_0 \\ B = b_0 \\ D = d_3 p^3 + d_2 p^2 + d_1 p + d_0 \\ R = r_1 p + r_0 \\ S = s_2 p^2 + s_1 p + d_0 \end{cases} \quad (24)$$

By using to the robust pole placement strategy [16], the polynomial D is written as [8]:

$$D = \left(p + \frac{1}{T_c}\right)\left(p + \frac{1}{T_f}\right)^2 \quad (25)$$

To accelerate the system, the following conditions were adopted:

$$D = (s - 5P_a)(s - 15P_a)^2 \quad (26)$$

With $P_C = -1/T_C$ pole of polynomial order C and $P_f = -1/T_f$ double pole of the polynomial filter F [8].

$$\begin{cases} P_c = 5P_a = -5\frac{R_l}{L_l} \\ T_c = \frac{1}{P_c} \\ T_f = \frac{1}{3}T_c \end{cases} \quad (27)$$

By identifying equations (24) and (27), coefficients of polynomial D are found and linked to the coefficients of R and S by the Sylvester Matrix [7, 8]. Thus, the parameters of the RST controller can be determined as follows:

$$\begin{cases} d_3 = a_1 s_2 \rightarrow s_2 = \frac{d_3}{a_1} \\ d_2 = a_1 s_1 \rightarrow s_1 = \frac{d_2}{a_1} \\ d_1 = a_0 s_1 + b_0 r_1 \rightarrow r_1 = \frac{d_1 - a_0 s_1}{b_0} \\ d_1 = b_0 r_0 \rightarrow r_0 = \frac{d_0}{b_0} \\ T = r_0 \end{cases} \quad (28)$$

V. SIMULATION INVESTIGATION AND DISCUSSION

The Fuzzy-PI and RST are used to control a matrix converter and a set of simulation runs is performed using SPS toolbox of Matlab/Simulink software for balanced, unbalanced and distorted grid voltage cases (Fig. 7). In the case of unbalanced grid, the amplitude of the input voltage of phase b is reduced to 20% relative to the phases a and c. The input filter parameters are calculated as in [11]. Bidirectional switches MOSFET are considered. The MC system's parameters are listed in Table III.

TABLE III. PARAMETERS SYSTEM

Parameters	Values
Input voltage phase to neuter RMS	$V_{im} = 220V$
Input frequency	$f_i = 50Hz$
Switching frequency	$f_s = 5KHz$
Input filter resistance	$R_f = 0.08\Omega$
Input filter inductance	$L_f = 30mH$
Input filter capacitor	$C_f = 25\mu F$
Load resistance	$R_l = 10\Omega$
Load inductance	$L_l = 55mH$

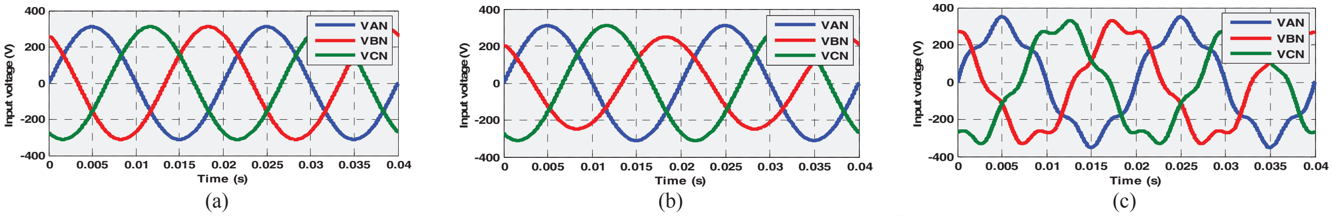

Figure 7. Grid voltage: (a) balanced; (b) unbalanced; and (c) distorted

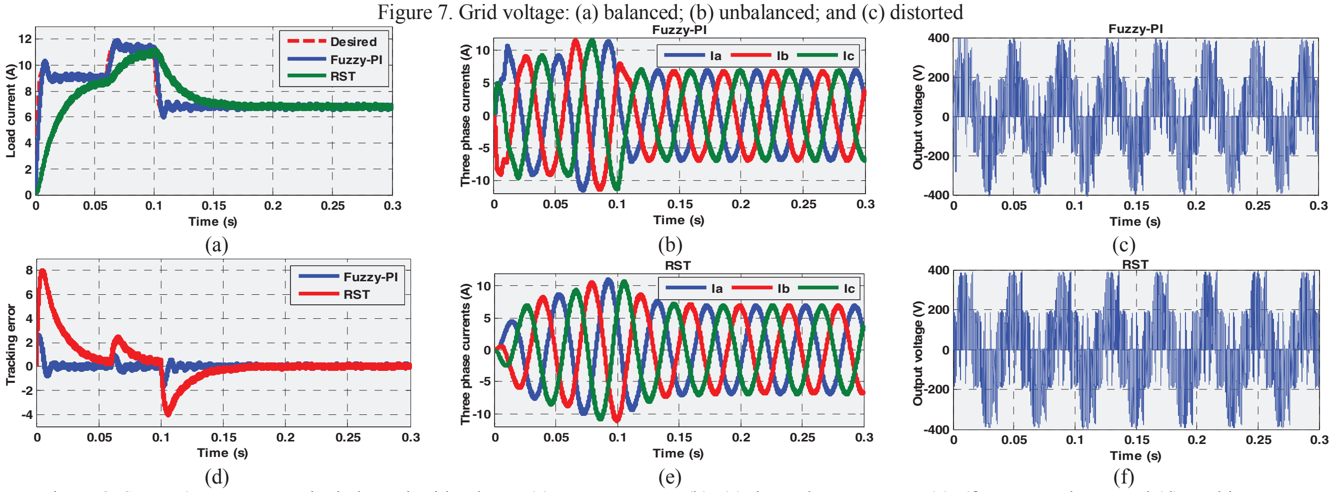

Figure 8. System's response under balanced grid voltage: (a) output current; (b)–(e) three phase currents; (c)–(f) output voltage; and (d) tracking error

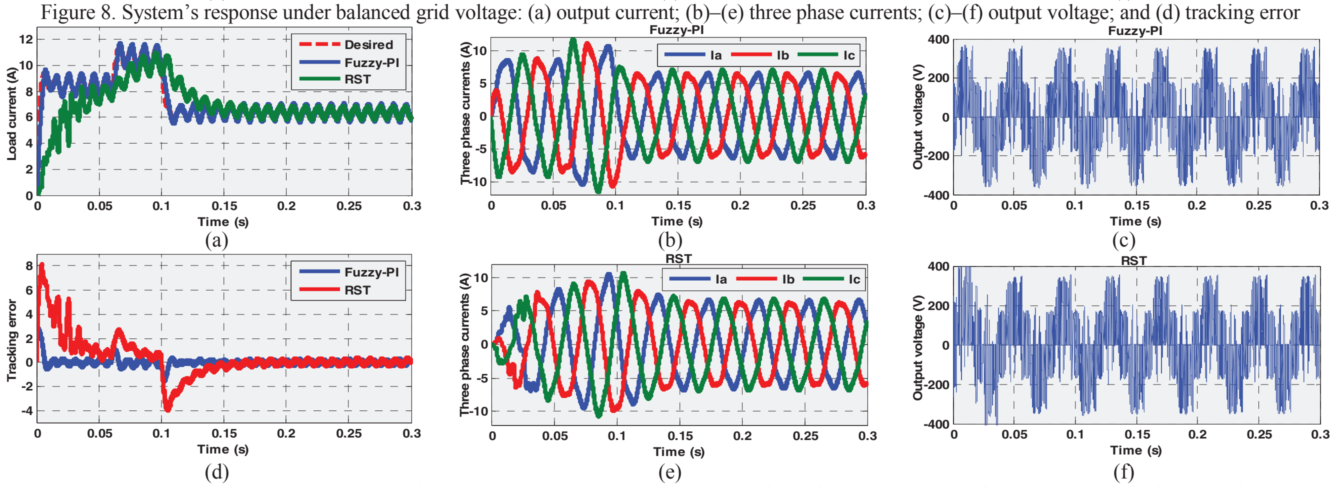

Figure 9. System's response under unbalanced grid voltage: (a) output current; (b)–(e) three phase currents; (c)–(f) output voltage; and (d) tracking error

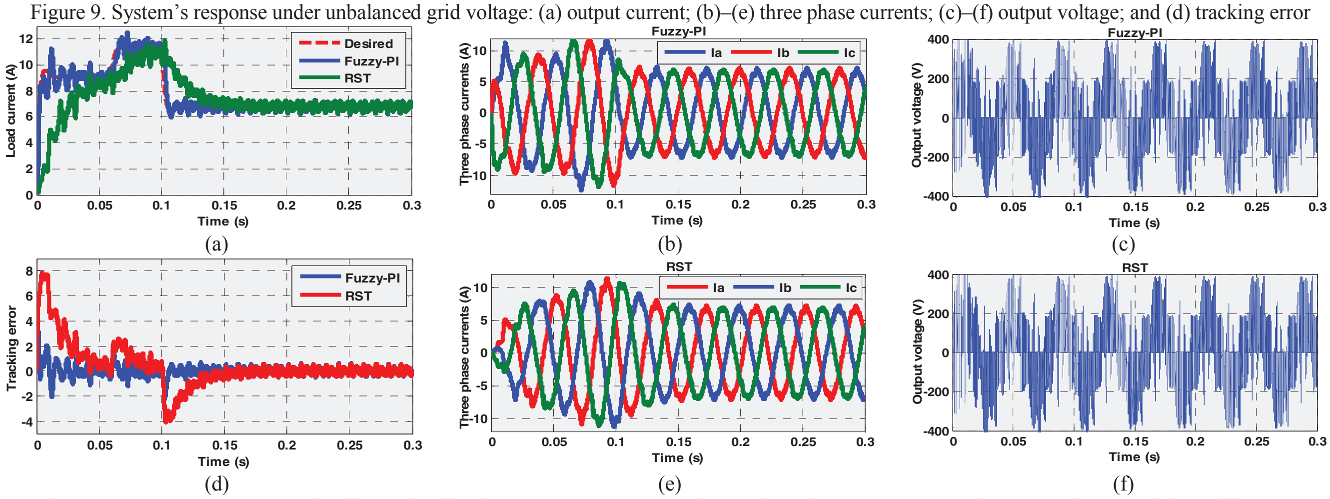

Figure 10. System's response under distorted grid voltage: (a) output current; (b)–(e) three phase currents; (c)–(f) output voltage; and (d) tracking error

TABLE IV. PERFORMANCE METRICS

	Balanced grid voltage			Unbalanced grid voltage			Distorted grid voltage		
	Fuzzy-PI	**RST**	**IMP%**	**Fuzzy-PI**	**RST**	**IMP%**	**Fuzzy-PI**	**RST**	**IMP%**
SSE	$4.4209e3$	$1.0128e6$	-99.57%	$4.2199e4$	$1.1031e6$	-96.17%	$6.8822e4$	$1.2520e6$	-94.50%
THD	1.95%	1.82%	6.67%	6.68%	4.95%	25.90%	3.78%	3.64%	3.70%

In Figure 8-b and 8-e, the voltage at the output of the MC is formed by a succession of pulse widths conversely proportional to the frequency of the reference voltage $f_o = 25\ \mathrm{Hz}$, and the RL load's current is almost sinusoidal with low THD values. In Figure 10-c and 10-f, the voltage at the output of the MC is formed by a succession of patterns which widths are proportional to the frequency of the reference voltage and the amplitude is $V_{im} = 300\mathrm{V}$. Table IV shows the values of THD and of the Sum Squared Error (SSE) for balanced, unbalanced and distorted voltage cases. The THD increases for the unbalanced grid unlike in the balanced case (Fig. 8). However, the output currents are almost balanced, but are distorted. With the RST strategy, the signal quality of load current is much better than Fuzzy-PI. Indeed, the THD is improved by 6.67% in the case of balanced grid and 3.70% in the distorted grid, while this improvement is around 25.90% in the case of unbalanced grid. In terms of the response of the system and the static error, the Fuzzy-PI controller achieves better results than RST controller as it can be seen in the Figure 8-a, 8-d, 9-a, 9-d, 10-a, and 10-d as well as in Table IV. Note that in the case of a balanced grid, it is noteworthy that the use of Fuzzy-PI leads to -99.57% improvement on the tracking error (Fig. 8-a, 8-d). Similar in the cases of balance and distorted gird, as it is shown in Figure 9-a, and 9-d. Fuzzy-PI outperforms again the RST by -96.17% improvement on error tracking. Furthermore, Fuzzy-PI shows a -94.50% improvements on error tracking (Fig. 10-a, 10-d).

VI. CONCLUSION

In this paper, a thorough theoretical modeling, analysis and comparison are presented for Fuzzy and RST control of MCs. Proportional and Integral coefficients of PI controller are calculated using fuzzy rules. As such, the fuzzy-PI adjusts continuously the controller's parameters depending on the error. Moreover, the use of the pole placement technique is also shown to determine the RST polynomial coefficients. Results for a balanced grid show lower load current THD as opposed to the unbalanced and distorted grid cases, which is expected. However, RST control shows better performance. It is noteworthy that nonlinear controllers tend to outperform these techniques at the expense of added complexity and computation. However, controllers are usually benchmarked against their counterparts with similar design complexity, which has been driving their use in the industry.

REFERENCES

[1] A. Dendouga, Contrôle des puissances active et réactive de la machine asynchrone à double alimentation (DFIM), Ph.D. in Electrical Engineering, University of Batna Algeria, 2010.

[2] F. P. A. Luis, Maximum Power Point Tracker of Wind Energy Generation Systems using Matrix Converters, Master degree thesis, of Electrical and Computer Engineering, Technical University of Lisbon, 2011.

[3] K. Hulusi, A. Ramazan, and D. Hüseyin, “A Novel Compensation Method Based on Fuzzy Logic Control for Matrix Converter under Distorted Input Voltage Conditions”, IEEE International Conference on Electrical Machines, , 2008.

[4] M. Venturini, and A. Alesina, “The generalised transformer: A new bidirectional sinusoidal waveform frequency converter with continuously adjustable input power factor”, IEEE Proc, Power electronics specialists Conf. PESC’80, pp. 242– 252, USA, 1980.

[5] M. E. O. Filho, E. R. Filho, K. E. B. Quindere, and J. R. Gazoli, “A Simple Current Control for Matrix Converter,” IEEE International Symposium on Industrial Electronics, pp. 2090-2094, 2006.

[6] G. Ram, S. and A. Lincoln, “Fuzzy adaptive PI controller for single input single output non-linear system”, ARPN Journal of Engineering and Applied, Sciences. Vol. 7, 10, pp. 1273–1280, 2012.

[7] Fatma Hachicha, Lotfi Krichen,” Performance Analysis of a Wind Energy Conversion System based on a Doubly-Fed Induction Generator”, IEEE 8th International Multi-Conference on Systems, Signals & Devices, pp. 978-984, 2011.

[8] A. Belabbes, B. Hamane, M. Bouhamida, A. Draou, and M. Benghanem, “Power Control of a Wind Energy Conversion System based on a Doubly Fed Induction Generator using RST and Sliding Mode Controllers”, International Conference on Renewable Energies and Power Quality (ICREPQ'12), Spain, March 2012.

[9] A. L. Oubelli, Mise En œuvre d’un modèle générique du convertisseur matriciel dans les environnements EMTP-RV et MATLAB-SIMULINK, Master's thesis, Ecole Polytechnique de Montréal, 2011.

[10] A. Boukadoum, T. Bahi, S. Oudina, Y. Souf A, and S. Lekhchine, “Fuzzy control adaptive of a matrix converter for harmonic compensation caused by nonlinear loads,” Energy Procedia 18, pp 715 -723, 2012.

[11] K. Ghedamsi, Contribution à la modélisation et la commande d’un convertisseur direct de fréquence Application à la conduite de la machine asynchrone, Ph.D. in Electrical Engineering, National Polytechnic School of Process Control Laboratory, Algeria, 2008.

[12] Luis Filipe Patricio Afonso, Maximum Power Point Tracker of Wind Energy Generation Systems using Matrix Converters. Master degree thesis in Electrical and Computer Engineering, Higher Technical Institue of Technical University of Lisbon, May 2011.

[13] Rodriguez, Silva E, Blaabjerk F, “Modelling, analysis and simulation of matrix converters“, Applications, vol. IA-21, no.6, pp. 1337-132, 1985.

[14] J. G. Slootweg, H. Polin der and, W. L. Kling, “Initialization of wind turbine models in power systems dynamic simulations,” IEEE Power Tech Conference, Porto, Portugal, Vol. 3, 6 pp, Sep. 2001.

[15] T.D. Mai, B.L. Mai, D.T. Pham, and H.P. Nguyen: “Control of doubly-fed induction generators using Dspace R&D controller board – an application of rapid control coordinated with Matlab/Simulink”, International Symposium on Electrical & Electronics Engineering, Track. 3, pp 302-307, October 2007.

[16] M. Bouhamida, M.A. Denai, “Robust Stabilizer of Electric Power Generator Using H∞ with Placement Constraints”, Jour. of Elec. Eng. (JEE), Vol. 56, No. 7-8, pp. 176-182, 2005.

[17] A. Hazzab, Commande des systèmes par logique floue, Réseau de neurones et Algorithmes géniques, PhD in Electrical Engineering, University Mohamed Boudiaf USTO Algeria, 2006.

[18] T. J. Porcyk, and E.H. Mamdani, “A linguistic self-organizing process controller,” Automatic, vol.15, pp.15 – 30, 1979.